

# MACCEPA 2.0: Adjustable Compliant Actuator with Stiffening Characteristic for Energy Efficient Hopping

Bram Vanderborght<sup>1,2</sup>, Nikos G. Tsagarakis<sup>1</sup>, Claudio Semini<sup>1</sup>,  
Ronald Van Ham<sup>2</sup>, Darwin G. Caldwell<sup>1</sup>

**Abstract**—The MACCEPA (Mechanically Adjustable Compliance and Controllable Equilibrium Position Actuator) is an electric actuator of which the compliance and equilibrium position are fully independently controllable and both are set by a dedicated servomotor. In this paper an improvement of the actuator is proposed where the torque-angle curve and consequently the stiffness-angle curve can be modified by choosing an appropriate shape of a profile disk, which replaces the lever arm of the former design. The actuator has a large joint angle, torque and stiffness range and these properties can be made beneficial for safe human robot interaction and the construction of energy efficient walking, hopping and running robots. The ability to store and release energy is shown by simulations on a 1DOF hopping robot. Its hopping height is much higher compared to a configuration in which the same motor is used in a traditional stiff setup. The stiffness of the actuator has a stiffening characteristic so the leg stiffness resembles more a linear stiffness as found in humans.

## I. INTRODUCTION

Compliant actuation gains interest in the robotics community due to its interesting properties regarding safe human-robot interaction (HRI) and energy-efficient locomotion. One approach is to use stiff actuation where the stiffness is software controlled by measuring joint angles/torques [1]. Problem is that for safe HRI the bandwidth of the software controlled stiffness is limited due to the time delay in the sensor data acquisition, the control loop and the motor inertia [2]. For energy-efficient locomotion as walking/running robots and walking prostheses, the drawback is that no energy can be stored [3]. Therefore passive compliant actuators are more favorable. Most well-known is the series elastic actuator (SEA) [4] where the stiffness of the spring is fixed, but its virtual stiffness can be adapted through the controller by measuring the length of the spring [5]. Other designs allow for both joint and stiffness control such as the MACCEPA [6], AMASC [3], VSA [7], DLR VS-Joint [8] or pneumatic muscles in an antagonistic setup [9] at the cost of an extra actuator. For a complete overview and classification of adaptable passive compliant actuators is referred to Van Ham et al. [10]. Whether these passive adaptable compliant actuators are better than compliant actuators with a fixed passive stiffness depends on the application and its required stiffness range and allowable weight. Due to the

lack of understanding of strategies to control the stiffness to meet safety or energy efficiency requirements, this question remains open and subject to further research. For safe HRI Bicchi et al. [11] proposed that when the robot moves slowly the joint can be made stiff for improved positional precision. For fast movements the stiffness can be decreased so the inertia of the motor is disconnected from the arm. An impact during both slow and fast movements will therefore result in a relatively low impact force. For walking, a stiffness control strategy is proposed in [12] where the idea was to fit the controllable stiffness to the natural stiffness of the desired trajectory. Au and Herr opted for SEA instead of adaptable compliant actuators for the powered ankle-foot prosthesis to reduce weight [13].

This paper presents an improvement of the former design of the MACCEPA [6]. The advantages of the MACCEPA actuator are that both the torque and stiffness are independently controllable, each by a dedicated motor, which can be optimized for a specific task. The device is not based on an antagonistic setup, which has drawbacks regarding energy efficiency [14]. The device uses a linear extension spring instead of a difficult to fabricate non-linear spring. Compared to other mechanisms, the design is simple and straightforward, which can be built with a strictly limited number of components. The actuator has both a large joint angle and stiffness range. The lever arm of the new design is replaced by a profile disk. Choosing an appropriate shape for the profile disk allows that the torque-angle curve can be modified and consequently the stiffness-angle curve compared to the old design. This freedom to choose the torque-angle curve can be used to make a stiffening spring required for eg hopping robots and prostheses as will be shown later. The working principle of the actuator will be shown by simulation of a 1DOF hopping robot actuated by a MACCEPA 2.0 actuator. It will be shown that much higher jumping heights can be achieved in comparison when a stiff actuator is used.

This paper is organized as follows. In section II the novel MACCEPA 2.0 is presented and compared with MACCEPA 1.0. In section III the actuator is implemented in a simulation of a 1DOF hopping robot to show the energy storage capabilities. Finally the conclusions are provided.

<sup>1</sup>Vrije Universiteit Brussel, Robotics & Multibody Mechanics Research Group Pleinlaan 2, 1050 Brussel, Belgium

<sup>2</sup>Italian Institute of Technology, Robotics, Brain and Cognitive Sciences Department, Via Morego 30, 16163 Genova, Italy  
bram.vanderborght@vub.ac.be,  
<http://mech.vub.ac.be/bram.htm>

## II. THE NOVEL ADJUSTABLE COMPLIANT ACTUATOR: MACCEPA 2.0

### A. Working principle of MACCEPA 1.0

An extensive description of the MACCEPA is provided in [6]. To understand and better show the differences with the new version a short overview of the MACCEPA is provided. Fig. 1 shows a schematic drawing of the MACCEPA. As can be seen, there are 3 bodies pivoting around one rotation axis. The left body in Fig. 1 is the reference body to which the generated actuator torque is applied and it can be considered as grounded. The smaller body is a lever arm rotating around the same rotation axis. A spring with spring constant  $k$  is placed between point  $c$  on the lever arm and a cable that runs around point  $b$ , a fixed point on the rotating right body. The cable is attached to a pretension mechanism. The angle

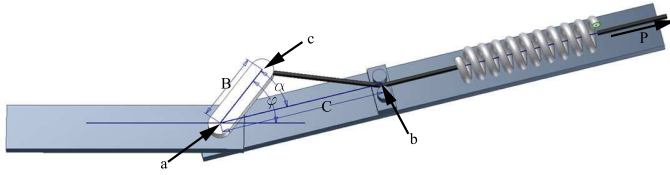


Fig. 1. Working principle of the MACCEPA actuator.

$\varphi$  between the smaller lever arm and the left body is set by a traditional position controlled actuator (e.g. a servomotor). Thus, this actuator defines the position of point  $c$ , where the spring is attached.  $P$  is the extension of the spring caused by pretensioning and equals to the total extension of the spring when  $\alpha = 0$ . The extension of the spring, equal to  $\sqrt{B^2 + C^2 - 2BC\cos(\alpha)} - (C - B) + P$ , has two independent causes: The variation of  $\alpha$  (the angle between the lever arm and the right body), and the setting of the pretension  $P$ . When  $\alpha$  differs from zero, the force due to the elongation of the spring will generate a torque  $T$  that tends to line up the right body with the lever arm. When the angle  $\alpha$  is zero -this is the equilibrium position- the spring will not generate any torque. Thus, the equilibrium position is determined by the value of  $\varphi$ , set by the servomotor.

This mechanism is an adjustable compliant actuator, since the equilibrium position can be controlled and a deviation from this equilibrium position is allowed. When pulling the actuator out of equilibrium, a returning torque is generated, which is a function of the applied angular deviation. To achieve adaptable compliance, the relation between the deviation and the reaction torque must be variable. This is realized by the pretension mechanism, which determines the length of the cable between the spring and point  $b$ , and thus the pretension of the spring. The pretension mechanism, based on a second servomotor with a spool, is located on the right arm. This pretension influences the torque exerted at certain angle  $\alpha$ , thus controlling the spring constant of the equivalent torsion spring used to model the device.

In [6] the torque  $T$  generated by a MACCEPA actuator is

calculated as:

$$T = kBC\sin(\alpha)\left(1 + \frac{P - (C - B)}{\sqrt{B^2 + C^2 - 2BC\cos(\alpha)}}\right) \quad (1)$$

The torque-angle and stiffness-angle curves are plotted in Fig. 2 and 3 as thin lines. The parameters used are  $k = 2520\text{N/m}$ ,  $B = 0.01\text{m}$  and  $C = 0.04\text{m}$ . The overall trend of the stiffness-angle curve is that the stiffness stays constant and then goes down so this is a weakening spring (the stiffness reduces when the joint is moved out of its equilibrium position). By changing the pretension different stiffnesses can be selected.

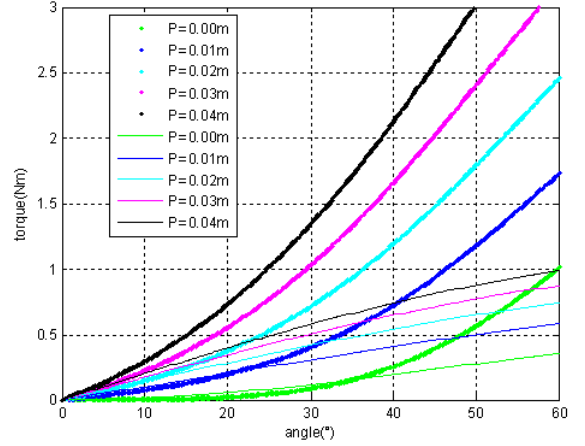


Fig. 2. Comparison of torque-angle ( $\alpha$ ) curve of MACCEPA 1.0 (thin line) and MACCEPA 2.0 (bold line) at different pretensions  $P$ .

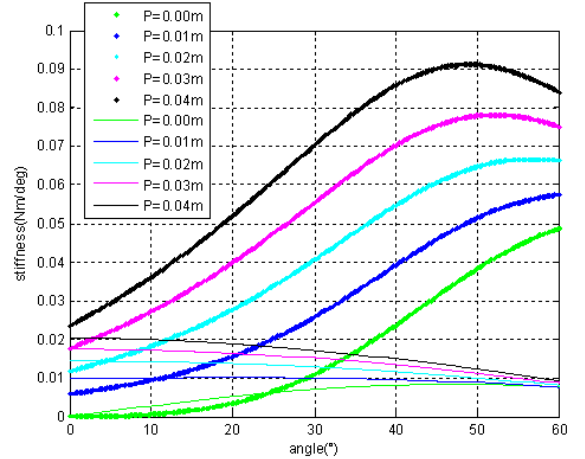


Fig. 3. Comparison of stiffness-angle ( $\alpha$ ) curve of MACCEPA 1.0 (thin line) and MACCEPA 2.0 (bold line) at different pretensions  $P$ .

### B. Working principle of novel MACCEPA 2.0

For certain applications a stiffening spring (being more compliant at low compressions and being stiffer at larger joint flexion) is more favorable like e.g. hopping robots and ankle-foot prostheses. To prevent a hopping robot during landing from reaching its end positions a stiffening spring is better. In human and animal locomotion a linear spring behavior is observed, meaning that a stiffening evolution is required for the joint. Seyfarth et al. [15] studied a three segment model and found that with linear stiffness in the

joints the system becomes unstable. A possible strategy to avoid this intrinsic instability is to use stiffening springs. When the torque-angle curve of a human ankle is studied then this behaves as a stiffening spring (segment 2-3 in Fig. 7) [16].

To be able to modify the torque-angle curve the MACCEPA is improved and the new version is called MACCEPA 2.0. A schematic drawing is provided in Fig. 4. The lever arm is replaced by a profile disk. When the position of the profile disk is changed by a servomotor or the joint is moved out of its equilibrium position, then the wire, held under tension by the spring, will be guided over the profile and causes the extension of the spring. Due to the force by the elongation of the spring, a torque will be generated. The torque depends on the shape of the profile. In the following example the profile consists of two disks with a constant radius. The idea of using a profile to shape the torque-angle curve was used by Wolf et al. [8] for the Variable Stiffness Joint (VS-Joint). This setup uses linear compression springs and cam rollers roll over the profile, while the MACCEPA 2.0 uses linear extension springs and a wire is guided over the profile.

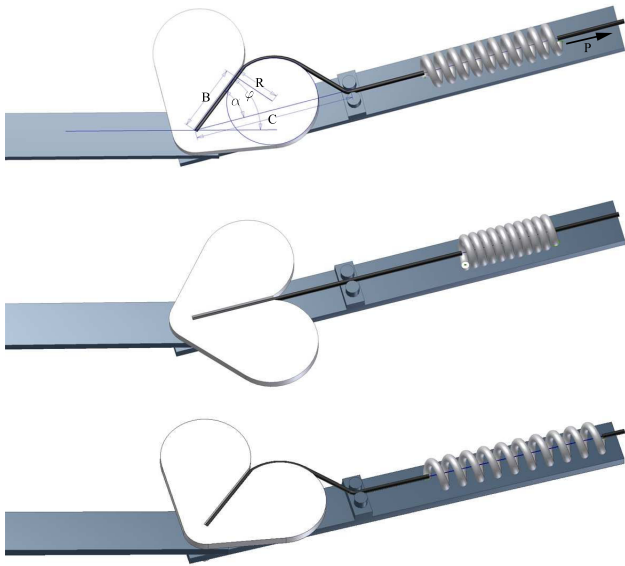


Fig. 4. Working principle of the novel MACCEPA 2.0. Top: Out of equilibrium position (generating torque) Middle: At equilibrium position (not generating torque) Bottom: Changed pretension.

The extension of the spring is determined by four lengths: The length  $B$  (similar as in the former design), the length  $D$  (the length where the wire is on the profile), the length  $E$  (the length of the wire between the profile  $d$  and the fixed point  $b$ ) and the pretension  $P$ . The extension of the spring, similar to MACCEPA 1.0, is due to the variation of  $\alpha$  (the angle between the profile disk and right body), and the setting of the pretension  $P$ . The profile disk is in the following example formed by a circle with radius  $R$ . The fixed point  $b$  is at a distance  $C$  from the rotation point  $a$ .

The calculation of the torques are straightforward geometrical calculations. A scheme with the necessary distances is provided in Fig. 5.  $I$  and  $H$  are the vertical and horizontal

part of the length  $A$  (the distance between the points  $o$  and  $b$ ).

$$\begin{aligned} I &= (C \cos(\alpha) - B) \\ H &= (R - C \sin(\alpha)) \\ A &= \sqrt{I^2 + H^2} \\ E &= \sqrt{A^2 - R^2} \end{aligned} \quad (2)$$

With those lengths the following angles can be calculated.  $\gamma$  is the angle between  $\overline{ob}$  and the vertical,  $\theta$  is the angle between  $\overline{od}$  and  $\overline{ob}$ ,  $\lambda$  between  $\overline{oc}$  and  $\overline{od}$  and  $\kappa$  between  $\overline{bd}$  and  $\overline{ba}$ .

$$\begin{aligned} \gamma &= \text{atan}(H/I) \\ \theta &= \text{atan}(E/R) \\ \lambda &= \frac{\pi}{2} - \gamma - \theta \\ \kappa &= \frac{\pi}{2} - \gamma - \theta - \alpha \end{aligned} \quad (3)$$

$J$  is the length of moment arm of the force  $F$ .

$$\begin{aligned} D &= R\lambda \\ J &= C \sin(\kappa) \end{aligned} \quad (4)$$

With this information it is possible to calculate the force  $F$  and the torque  $T$ . The stiffness  $K$  is numerically calculated by taking the derivative of the the torque  $T$  with respect to the angle  $\alpha$ .

$$\begin{aligned} F &= k(-C + B + D + E + P) \\ T &= FJ \end{aligned} \quad (5)$$

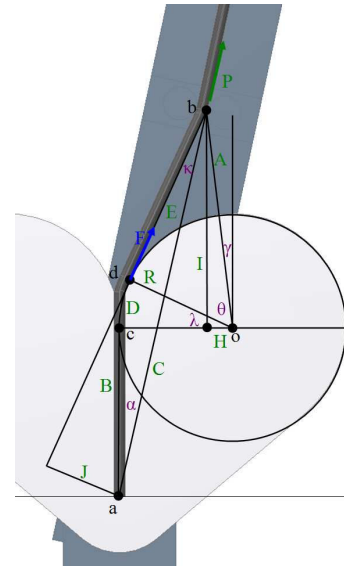


Fig. 5. Scheme of necessary distances and angles to calculate torque and stiffness.

The torque-angle and stiffness-angle curves are plotted in Fig. 2 and 3 with similar parameters as the former design  $k = 2520 \text{ N/m}$ ,  $B = 0.01 \text{ m}$ ,  $R = 0.015 \text{ m}$  and  $C = 0.04 \text{ m}$  (see Fig. 6 for physical realization). By changing the pretension different stiffnesses can be selected. The overall trend is that the stiffness increases with increasing angle  $\alpha$ . This is a stiffening spring as was desired (the stiffness increases when the joint is moved out of its equilibrium position).

By choosing other profile shapes the torque-angle curve can be adapted. Moreover it is possible to design two different shapes of the profile disk so a different stiffness is obtained depending on rotation direction.

The stiffness of the spring  $k$  scales linearly the torque and stiffness. With the length  $B$ , the stiffness in the equilibrium position is adapted. The radius  $R$  influences the slope at which the stiffness increases when going out of the equilibrium position. The length  $C$  has a minimal influence on the torque characteristics. It must be chosen so the profile disk can rotate freely and not too big so there is enough space available for the extension of the spring.

### III. IMPLEMENTATION IN HOPPING ROBOT

Adaptable compliant actuator can be used for walking robots to exploit the natural dynamics of the system to reduce the energy consumption. In [12] a compliance controller is developed to tune the stiffness of the actuator on the natural stiffness of the desired trajectory. In this section the capabilities of a compliant actuator to store and release energy will be shown to reduce the energy consumption of a hopping robot. Robots actuated with stiff actuators soon reach the limits of the system because the impact shocks need to be kept small [17]. During each hop all the potential and kinetic energy is lost during the inelastic collision with the ground [3], which has to be recovered by draining the batteries of the electric motors. A study on the HRP1 robot showed that motors need to be 28-56 times more powerful without increasing the weight of the robot to make the robot run at  $10\text{km}/\text{h}$ . Moreover this will consume 10 times more energy than a human [18].

There is biological evidence that a common theme among all runners is spring-like behavior [19]. The model often used is the SLIP (Spring Loaded Inverted Pendulum) model to describe the motion of the Center of Mass (CoM) of the robot. Raibert studied different running robots [20] [21]. These famous hopping robots were driven by pneumatic and hydraulic actuators and performed various actions including somersaults [22]. Key factor was the spring mechanism to store kinetic energy during running cycles. Hurst et Rizzi [3] built the BiMASC (Biped with Mechanically Adjustable Series Compliance), actuated by the AMASC (Actuator with Mechanically Adjustable Series Compliance) where the leg length, leg stiffness and leg angle were controllable. They abandoned the idea of using antagonistic setup of muscles: They calculated that energy storage capacity is strongly reduced in the antagonistic setup, because energy needs to be transferred from one spring and put in the other spring instead of releasing it to the joint. Also the structure had to be strong enough for the high internal forces. Their ECD (Electric Cable Differential) Leg performed successful hopping experiments; here the leg stiffness is only adaptable by software control. In another study [14] is described that an antagonistic setup of two SEA is energy uninteresting compared to a MACCEPA actuator.

To test the novel MACCEPA 2.0 and study the influence of controllable stiffness for hopping robots the 1DOF hopping

robot Chobino1D (Fig. 6) is under construction. The parts are produced using the Fused Deposition Modeling (FDM) rapid prototyping technology. Currently is investigated how to make the different ABS parts strong and light enough to withstand the high forces during hopping. To focus on energy efficiency and to be able to omit stability problems the simplest hopper was chosen. The knee is actuated and the hip and ankle are passive joints connected to a slider. The lengths of the links are  $0.2\text{m}$ . Both the equilibrium position and the pretension are controlled by a Hitec HSR-5990TG coreless digital robot servo (3Nm stall torque). The torque of the motor is transferred to the profile disk through a cable transmission system. The profile disk has parameters as in Fig. 2 and 3. A potentiometer measures the knee joint angle.

This is an interesting example because the jumping height of the robot is determined by the take-off velocity. Generally, the rotational speed of a DC motor is proportional to the voltage applied to it and consequently limited. By using the energy storage capabilities of the springs this maximum speed will be increased.

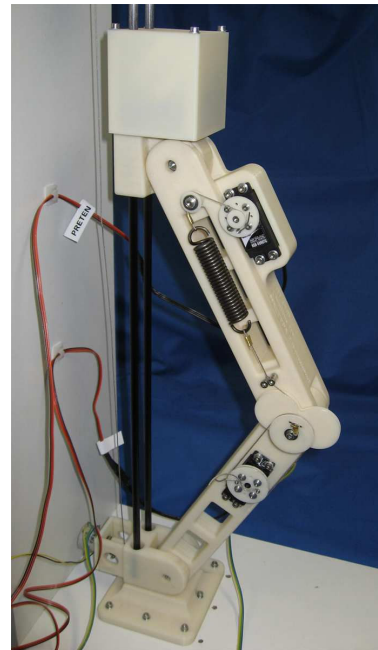


Fig. 6. Picture of Chobino1D, a 1DOF hopping robot actuated with the MACCEPA 2.0.

#### A. Hopping simulations

This section discusses the simulations of hopping experiments. The mass of the robot ( $0.7\text{kg}$ ) is considered to be located in the hip and no friction is assumed. A simple trajectory is imposed for the motor controlling the angle of the profile disk ( $\varphi$ ) as depicted in Fig. 8. The pretension, when the leg is in contact with the ground, is held fixed. The angle  $\phi$  is the knee joint angle and equals  $\varphi - \alpha$ . First the equilibrium position is increased by the motor to bend the knee and the hip of robot moves down. At  $t = 0.20\text{s}$  the equilibrium is changed from  $30^\circ$  to  $0^\circ$  in  $0.175\text{s}$ , with a

velocity of  $171^\circ/s$ . The knee angle goes much higher than the maximum angle of the equilibrium position and then goes very fast to zero. The knee bends deep and then goes to a complete stretched position with a velocity much higher than the speed of the servomotor. If the same velocity of  $171^\circ/s$  is used as the velocity of a stiff actuator, then the speed of the robot varies between  $0.6m/s$  (completely bent) and  $0m/s$  (completely stretched). The highest speed is taken as take off-speed  $\dot{Y}^{TO}$  to calculate the jumping height  $\Delta Y$ .

$$\Delta Y = \frac{\dot{Y}^{TO}}{2g} = \frac{0.6^2}{2g} = 0.018m \quad (6)$$

The vertical position of the hip is shown in Fig. 9. The robot attains a height of  $0.5m$ , so the jumping height is  $\Delta Y = 0.5m - 0.4m = 0.1m$ . By using a compliant actuator the jumping height can be increased several times compared to a stiff actuator. Reason is that due to the difference in equilibrium position and joint angle, energy is stored in the spring as can be seen in Fig. 10. The green line is the sum of the kinetic and potential energy of the mass of the robot, which decreases because the robot first bends and then reaches a constant level in the aerial phase. The light blue line is the total energy in the system and is supplied by the energy of the motor (red line) and by changing the pretension. The motor energy (red line) equals the total energy in the system (light blue line) in the beginning because the pretension is not changed during the first two hops. The supplied energy increases gradually until the constant level. The spring is no energy source, only an energy buffer, so all the energy required to jump comes from the motor. The blue line is the energy of the spring, which first increases by taking the energy when the robot bends the knee and by absorbing energy from the motor, in the second phase it releases its energy and puts it into the robot until there is no energy left in the spring at lift-off. As depicted in Fig. 11 about the power, the motor does not need to give such a high power output as the robot requires. The power is spread out over the complete push-off motion.

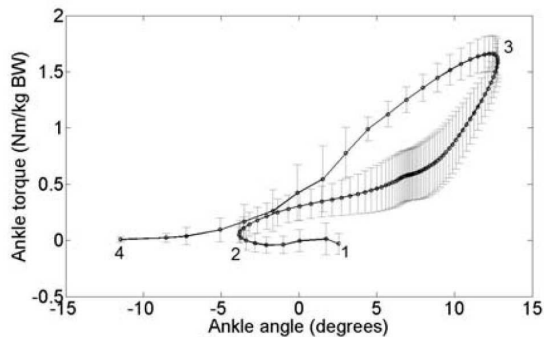


Fig. 7. Ankle torque vs. ankle angle in normal walking (Data are averaged from clinical gait tests on 52 healthy subjects) [16].

When the stiffness is changed in the aerial phase, the jumping height will remain the same because no extra energy is injected in the mass of the robot, but in the spring. At  $t = 1.0s$  the pretension  $P$  is changed from  $0.010m$  to

$0.015m$  and at  $t = 1.89s$  to  $0.02m$ . The frequency will change because the time the robot is on the ground changes. When the stiffness increases, the knee bends less (Fig. 8).

An interesting curve is the torque-angle relation shown in Fig. 12. Phase  $a$  to  $b$  is the period from  $t = 0s$  to  $t = 0.2s$ ,  $c$  is at  $t = 0.38s$ . Point  $d$  is at maximum bending of the knee. The area under line  $a-d$  is the stored energy in the spring. The area under line  $d-c$  equals the total energy gained by the hopping robot at take-off. The area in the loop  $a-b-d-c$  is the energy supplied by the motor. When compared to the period 2-3 of the torque-angle curve of human walking (Fig. 7) one can see the close resemblance while the controller is a simple open loop desired trajectory for the equilibrium position.

Lines  $c-e$ ,  $c-f$  and  $c-g$  are the passive jumping motions without loop area because no energy injection or energy loss (simulation with ideal situation). The higher the stiffness the less knee bending is observed as expected. The area under the curve is the energy stored and released by the spring, impossible to attain by using actuators with stiff actuation.

Another similar experiment showing the energy storage capabilities of a compliant actuator was shown by Wolf et al. [8]. They used their novel VS-Joint to throw a ball much further compared to a similar joint actuated by stiff actuator.

#### IV. CONCLUSION

A novel version of the MACCEPA actuator is proposed where the torque-angle curve and consequently the stiffness-angle curve can be modified by choosing an appropriate shape of a profile disk. The advantage of the setup is that the design is simple, linear springs can be used and the control of equilibrium position and pretension is independent. The actuator has both a large joint angle and stiffness range. The actuator is implemented in a simulation of a 1DOF hopping robot to show its energy storing capabilities. Its hopping height is higher compared to a configuration in which the same motor is used in a classical stiff setup. By changing the spring pretension different hopping frequencies can be obtained.

Future works consist in finishing the real robot Chobino1D, controlling equilibrium position and pretension for obtaining different hopping heights and frequencies. Special focus will be placed on measuring the energy loss due to friction and impact and refeed this lost energy into the system by controlling the angle  $\varphi$  so that the robot can jump continuously with minimal energy consumption.

#### V. ACKNOWLEDGMENTS

The author Bram Vanderborcht is a post-doc researcher with a grant from the Fund for Scientific Research-Flanders (Belgium)(FWO). This work has been funded by the European Commissions 7th Framework Program as part of the project VIATORS under grant no. 231554.

#### REFERENCES

- [1] A. Albu-Schaffer, O. Eiberger, M. Grebenstein, S. Haddadin, C. Ott, T. Wimbock, S. Wolf, and G. Hirzinger, "Soft robotics," *IEEE Robotics & Automation Magazine*, vol. 15, no. 3, pp. 20-30, September 2008.

- [2] M. Zinn, O. Khatib, B. Roth, and J. Salisbury, "Playing it safe [human-friendly robots]," *IEEE Robotics & Automation Magazine*, vol. 11, no. 2, pp. 12–21, June 2004.
- [3] J. W. Hurst and A. A. Rizzi, "Series compliance for robot actuation: Application on the electric cable differential leg," *IEEE Robotics & Automation Magazine*, vol. 15, no. 3, pp. 42–51, September 2008.
- [4] G. A. Pratt and M. M. Williamson, "Series elastic actuators," in *IEEE International Workshop on Intelligent Robots and Systems (IROS 1995)*, Pittsburg, USA, 1995, pp. 399–406.
- [5] T. Sugar, "A novel selective compliant actuator," *Mechatronics*, vol. 12, no. 9, pp. 1157–1171, November 2002.
- [6] R. Van Ham, B. Vanderborght, M. Van Damme, B. Verrelst, and D. Lefeber, "MACCEPA, the Mechanically Adjustable Compliance and Controllable Equilibrium Position Actuator: Design and Implementation in a Biped Robot," *Robotics and Autonomous Systems*, vol. 55, no. 10, pp. 761–768, October 2007.
- [7] A. Bicchi and G. Tonietti, "Fast and soft arm tactics: Dealing with the safety-performance trade-off in robot arms design and control," in *IEEE Robotics and Automation Magazine*, vol. 11, no. 2, 2004, pp. 22–33.
- [8] S. Wolf and G. Hirzinger, "A new variable stiffness design: Matching requirements of the next robot generation," in *IEEE International Conference on Robotics and Automation (ICRA 2008)*, May 2008, pp. 1741–1746.
- [9] B. Vanderborght, R. Van Ham, B. Verrelst, M. Van Damme, and D. Lefeber, "Overview of the lucy project: Dynamic stabilization of a biped powered by pneumatic artificial muscles," *Advanced Robotics*, vol. 22, no. 25, pp. 1027–1051, 2008.
- [10] R. Van Ham, S. Thomas, B. Vanderborght, K. Hollander, and D. Lefeber, "Review of actuators with passive adjustable compliance / controllable stiffness for robotic applications," *IEEE Robotics and Automation Magazine*, p. accepted, 2009.
- [11] A. Bicchi, G. Tonietti, M. Bavaro, and M. Piccigallo, "Variable stiffness actuators for fast and safe motion control," in *Int. Symposium Robotics Research*, 2003, pp. 100–110.
- [12] B. Vanderborght, B. Verrelst, R. Van Ham, M. Van Damme, P. Beyl, and D. Lefeber, "Development of a compliance controller to reduce energy consumption for bipedal robots," *Autonomous Robots*, vol. 24, no. 4, pp. 419–434, May 2008.
- [13] S. Au and H. Herr, "Powered ankle-foot prosthesis," *IEEE Robotics & Automation Magazine*, vol. 15, no. 3, pp. 52–59, September 2008.
- [14] B. Vanderborght, T. Sugar, R. Van Ham, K. Hollander, and D. Lefeber, "Comparison of mechanical design and energy consumption of adaptable passive compliant actuators," *International Journal of Robotics Research*, vol. 28, no. 1, pp. 90–103, January 2008.
- [15] A. Seyfarth, H. Geyer, R. Blickhan, S. Lipfert, J. Rummel, Y. Minekawa, and F. Iida, *Fast Motions in Biomechanics and Robotics*. Springer Berlin / Heidelberg, 2006, vol. 340, ch. Running and walking with compliant legs, pp. 383–401.
- [16] R. Versluis, A. Desomer, G. Lenaerts, O. Pareit, B. Vanderborght, G. Van der Perre, L. Peeraer, and D. Lefeber, "A biomechatronic transtibial prosthesis powered by pleated pneumatic artificial muscles," *International Journal Modelling, Identification and Control*, vol. 4, no. 4, pp. 394–405, 2008.
- [17] S. Kajita, T. Nagasaki, K. Kaneko, K. Yokoi, and K. Tanie, "A Running Controller of Humanoid Biped HRP-2LR," in *IEEE International Conference on Robotics and Automation (ICRA 2005)*, 2005, pp. 616–622.
- [18] S. Kajita, T. Nagasaki, K. Yokoi, K. Kaneko, and K. Tanie, "Running pattern generation for a humanoid robot," in *IEEE International Conference on Robotics and Automation (ICRA 2002)*, vol. 3, 2002, pp. 2755–2761.
- [19] R. M. Alexander, *Exploring Biomechanics: Animals in Motion*. New York: Scientific American Library, 1992.
- [20] M. Raibert, H. J. Brown, and M. Chepponis, "Experiments in balance with a 3D one-legged hopping machine," *International Journal of Robotics Research*, vol. 3, no. 2, pp. 75–92, 1984.
- [21] M. Raibert and H. J. Brown, "Experiments in balance with a 2D one-legged hopping machine," *Journal of Dynamic Systems, Measurement and Control*, vol. 106, pp. 75–81, 1984.
- [22] R. Playter and M. Raibert, "Control of a biped somersault in 3D," in *IEEE/RSJ International Conference on Intelligent Robots and Systems (IROS 1992)*, Raleigh, NC, USA, 1992, pp. 582–589.

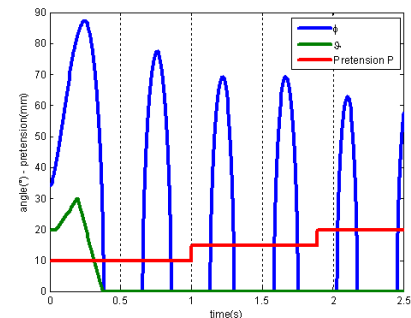


Fig. 8. Equilibrium position, knee joint angle and pretension.

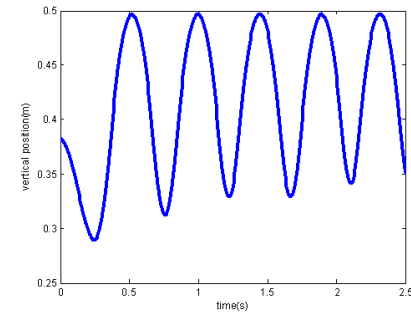


Fig. 9. Vertical position robot.

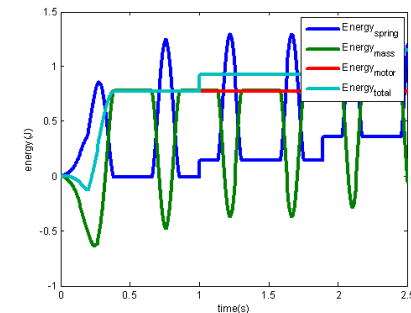


Fig. 10. Energy in spring, mass of robot, delivered by motor and total in system.

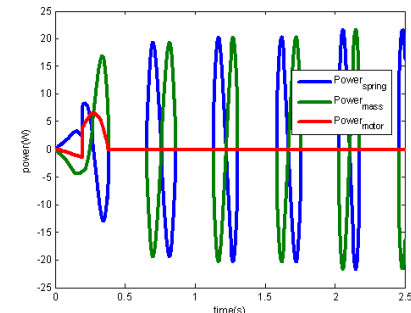


Fig. 11. Power delivered by robot, motor and spring.

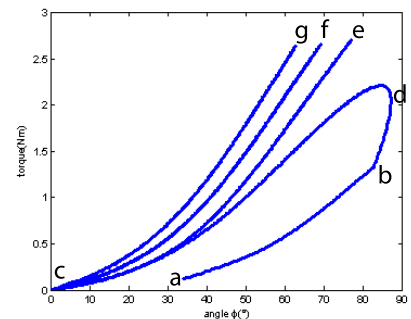


Fig. 12. Torque-angle curve for knee angle.